



University of Wisconsin - Madison

MAD/PH/851

October 1994

Relativistic Flux Tube Model Calculation of the Isgur-Wise Function

M. G. Olsson and Siniša Veseli

Department of Physics, University of Wisconsin, Madison, WI 53706

Abstract

The Relativistic Flux Tube model is used to calculate of the Isgur-Wise functions describing the exclusive semileptonic decays of \bar{B} and \bar{B}_s mesons. The light quark mass dependence is investigated and the predicted universal function agrees well with the results of lattice simulations, and with the experimental data. Recent experimental measurements of the $\bar{B} \rightarrow D^* l \bar{\nu}_l$ decay distribution yield the CKM element $V_{bc} = 0.035 \pm 0.001$. The IW function slope and second derivative at the zero recoil point are predicted to be $\xi'(1) = -0.93 \pm 0.04$ and $\xi''(1) = 1.7 \pm 0.1$ for a range of light quark masses. The importance of including higher derivatives in analyses of experiment is emphasized.

1 Introduction

In the heavy quark limit (mass of the heavy quark $m_Q \rightarrow \infty$) all the non-perturbative, strong interaction physics for semileptonic $\bar{B} \rightarrow Dl\bar{\nu}_l$ and $\bar{B} \rightarrow D^*l\bar{\nu}_l$ decays (and corresponding \bar{B}_s decays), can be parametrized in terms of a single universal function [1], known as the Isgur-Wise (IW) function. Knowledge of the IW function is essential in all calculations that lead to numerical values of branching ratios of semileptonic decays and of the V_{cb} element of the CKM matrix. A reliable calculation of the IW function from first principles is still beyond our power, although recent efforts using lattice QCD are very encouraging. A variety of different meson models make specific predictions for the IW function. Since these model results vary widely, the IW prediction can be considered to be a sensitive gauge of model validity.

The relativistic flux tube (RFT) model shows promise to provide a realistic description of all meson states. The RFT model is in essence a description of dynamical confinement [2]-[6]. For slowly moving quarks rigorous QCD relativistic corrections [7]-[9] clearly demonstrate that the scalar confinement potential picture is incorrect [3, 9]. On the other hand, the RFT model dynamics is consistent with both spin-dependent [4, 10, 11] and spin-independent [2, 3] QCD expectations. In this paper we examine the RFT model predictions for IW functions. We find here that the spinless light degrees of freedom model is in excellent agreement with both experiment and with fundamental QCD expectations.

We begin by a brief review of the RFT formalism. In Section 3 we outline the general calculation of the IW function and its derivatives at the zero recoil point. Our numerical results and conclusions are given in Section 4. Here we evaluate the RFT predictions for the IW function and examine its dependence on the light quark

mass. We determine the V_{cb} CKM element and branching fractions for various exclusive semi-leptonic decays and test the shape of the predicted IW function. Finally we note that the RFT prediction for the slope at the zero recoil point is in good agreement with present lattice simulation results.

2 RFT model in the heavy quark limit

In the limit $m_{\bar{Q}} \rightarrow \infty$ the quantized equations of the spinless RFT model with light quark mass m_q are [5, 6]

$$\frac{\sqrt{l(l+1)}}{r} = \frac{1}{2}\{W_r, \gamma_\perp v_\perp\} + a\{r, f(v_\perp)\}, \quad (1)$$

$$H_q = H - m_{\bar{Q}} = \frac{1}{2}\{W_r, \gamma_\perp\} + \frac{a}{2}\{r, \frac{\arcsin v_\perp}{v_\perp}\} + V(r). \quad (2)$$

Here H_q is Hamiltonian of the light degrees of freedom (LDF), with the short range potential

$$V(r) = -\frac{\kappa}{r}, \quad (3)$$

and

$$W_r = \sqrt{p_r^2 + m_q^2}, \quad (4)$$

$$\gamma_\perp = \frac{1}{\sqrt{1 - v_\perp^2}}, \quad (5)$$

$$f(v_\perp) = \frac{1}{4v_\perp} \left(\frac{\arcsin v_\perp}{v_\perp} - \frac{1}{\gamma_\perp} \right). \quad (6)$$

It is assumed that v_\perp is Hermitian, and the symmetrization (curly brackets in (1) and (2)) then yields a Hermitian Hamiltonian.

The solution of the energy eigenvalue equation

$$H_q \Phi = E_q \Phi \quad (7)$$

required the development of methods to eliminate the a-priori unknown operator v_\perp and also to address the solution of operator equations in which functions of both p_r and r appear. Our approach [2, 5, 6] employs the Galerkin method [12] in which a truncated basis set is used to transform the operator equations (1-7) into finite matrix equations. The resulting matrix equations describe the motion of a light quark with radial momentum p_r and perpendicular velocity v_\perp relative to a static heavy antiquark. In order to solve for the eigenvalues of the Hamiltonian, one first solves the angular momentum equation (1) for the v_\perp matrix, and then diagonalizes the H_q matrix (2) as discussed in detail in references [5, 6].

Since there is no spin-orbit coupling in the above model, we can write our wave function (describing the LDF in the meson rest frame) as a product of the orbital wave function and the light quark spinor as

$$\Psi_{H_{\bar{Q}}}^{(0)}(x) = \Phi_{\alpha LM_L}^{(0)}(\mathbf{x}) \phi_{m_{s_q}}^{(0)} e^{-iE_q t}. \quad (8)$$

Here, $H_{\bar{Q}}$ represents all quantum numbers of the LDF, and the superscript 0 denotes the rest frame of a meson.

3 Decays $H_{\bar{b}} \rightarrow H_{\bar{c}} l \bar{\nu}_l$ and the IW functions in the spinless RFT model

For heavy-light mesons, the spin of the heavy quark $\mathbf{s}_{\bar{Q}}$ and the spin of the light antiquark \mathbf{s}_q decouple as $\frac{1}{m_{\bar{Q}}}$, and in the limit $m_{\bar{Q}} \rightarrow \infty$ they are conserved separately by the strong interactions. Because of this, hadrons containing a single heavy quark can be simultaneously assigned the quantum numbers $(s_{\bar{Q}}, m_{s_{\bar{Q}}})$ and (s_q, m_{s_q}) , and matrix element of the hadron current describing semileptonic decay can be expressed by the free heavy quark current and the IW function.

Except for a trivial kinematical factor, the IW function $\xi(\omega)$ is defined [13, 14] as the overlap of the wave functions describing the light degrees of freedom in the

two mesons, i.e.

$$\xi(\omega) = \sqrt{\frac{2}{\omega + 1}} \langle \Psi_{H_{\bar{c}}} | \Psi_{H_{\bar{b}}} \rangle . \quad (9)$$

Here, if the meson velocity in the lab frame is \mathbf{v} , the wave function describing its LDF is

$$\Psi_{H_{\bar{Q}}}(x') = S(\mathbf{v}) \Psi_{H_{\bar{Q}}}^{(0)}(x) , \quad (10)$$

with $x' = \Lambda^{-1}(\mathbf{v})x$ being the lab frame, x the rest frame of the particle, and $S(\mathbf{v})$ is the wave function Lorentz boost.

Since the IW function is Lorentz invariant, we can choose any frame to calculate it. Particularly convenient is the modified Breit frame [13, 14], where the two particles move along the z-axis with equal and opposite velocities. Denoting velocity of $H_{\bar{c}}$ as \mathbf{v} , by the use of (10) the overlap takes the form

$$\begin{aligned} \langle \Psi_{H_{\bar{c}}} | \Psi_{H_{\bar{b}}} \rangle &= \langle \Phi_{H_{\bar{c}}} | \Phi_{H_{\bar{b}}} \rangle \langle \phi_{H_{\bar{c}}} | \phi_{H_{\bar{b}}} \rangle \\ &= \langle \phi_{H_{\bar{c}}} | \phi_{H_{\bar{b}}} \rangle \int d^3x' \Phi_{H_{\bar{c}}}^\dagger(x') \Phi_{H_{\bar{b}}}(x')|_{t'=0} \\ &= \langle \phi_{H_{\bar{c}}}^{(0)} | S^\dagger(\mathbf{v}) S(-\mathbf{v}) | \phi_{H_{\bar{b}}}^{(0)} \rangle \int d^3x' \Phi_{H_{\bar{c}}}^{(0)\dagger}(x_+) S^\dagger(\mathbf{v}) S(-\mathbf{v}) \Phi_{H_{\bar{b}}}^{(0)}(x_-)|_{t'=0} . \end{aligned} \quad (11)$$

In this expression x_+ and x_- denote the rest frames of $H_{\bar{c}}$ (moving in the +z direction) and $H_{\bar{b}}$ (moving in the -z direction), respectively. Using the fact that Lorentz boosts are real, i.e. $S^\dagger(\mathbf{v}) = S(\mathbf{v}) = S^{-1}(-\mathbf{v})$, the boost factors cancel out. The overlap of spin part of the wave functions will just give us $\delta_{m_{sq}^{H_{\bar{c}}}, m_{sq}^{H_{\bar{b}}}}$, which we suppress in the following, and we are left with

$$\langle \Psi_{H_{\bar{c}}} | \Psi_{H_{\bar{b}}} \rangle = \int d^3x' \Phi_{H_{\bar{c}}}^{(0)\dagger}(x_+) \Phi_{H_{\bar{b}}}^{(0)}(x_-)|_{t'=0} . \quad (12)$$

Denoting $v = |\mathbf{v}|$ and $\gamma = \frac{1}{\sqrt{1-v^2}}$, and using

$$x_\pm|_{t'=0} = \Lambda(\pm\mathbf{v})x'|_{t'=0} = (\mp\gamma v z', x', y', \gamma z') , \quad (13)$$

we obtain

$$\begin{aligned} \langle \Psi_{H_{\bar{c}}} | \Psi_{H_{\bar{b}}} \rangle &= \int d^3x' \Phi_{H_{\bar{c}}}^{(0)\dagger}(-\gamma v z', x', y', \gamma z') \Phi_{H_{\bar{b}}}^{(0)}(+\gamma v z', x', y', \gamma z') \\ &= \int d^3x' \Phi_{H_{\bar{c}}}^{(0)\dagger}(x', y', \gamma z') \Phi_{H_{\bar{b}}}^{(0)}(x', y', \gamma z') e^{-2iE_q\gamma v z'} , \end{aligned} \quad (14)$$

since the energies of the light degrees of freedom are the same in both hadrons. Finally, after rescaling the z' coordinate ($z' \rightarrow \frac{1}{\gamma}z'$), renaming integration variables, and noting kinematical identities

$$\gamma = \sqrt{\frac{w+1}{2}} , \quad (15)$$

$$v = \sqrt{\frac{\omega-1}{\omega+1}} , \quad (16)$$

valid in the Breit frame, the IW function becomes [14]

$$\xi(\omega) = \frac{2}{\omega+1} \int d^3x \Phi_{H_c}^{(0)\dagger}(\mathbf{x}) \Phi_{H_b}^{(0)}(\mathbf{x}) e^{-2iE_q v z} . \quad (17)$$

By spherical symmetry, and since we are interested here only in s-waves, the orbital wave function has the form

$$\Phi_{\alpha 0}(\mathbf{x}) = R_{\alpha 0}(r) \frac{1}{\sqrt{4\pi}} . \quad (18)$$

For the calculation of the IW function we need to evaluate integral of the form

$$\frac{1}{4\pi} \int d^3x R_{\alpha' 0}^*(r) R_{\alpha 0}(r) e^{-2iE_q v z} . \quad (19)$$

Using

$$e^{-ikz} = \sum_{l=0}^{\infty} (2l+1)(-i)^l j_l(kr) \sqrt{\frac{4\pi}{2l+1}} Y_{l0} , \quad (20)$$

and orthonormality of the spherical harmonics, one easily obtains the IW function in the form

$$\xi(\omega) = \frac{2}{\omega+1} \langle j_0(2E_q \sqrt{\frac{\omega-1}{\omega+1}} r) \rangle , \quad (21)$$

where

$$\langle A \rangle = \int_0^\infty dr r^2 R_{\alpha' 0}(r) A(r) R_{\alpha 0} . \quad (22)$$

The result (21) can also be used to obtain derivatives of the IW function at the zero recoil point ($\omega = 1$). Explicit results for the first two such derivatives are

$$\xi'(1) = -\left(\frac{1}{2} + \frac{1}{3}E_q^2\langle r^2 \rangle\right), \quad (23)$$

$$\xi''(1) = \frac{1}{2} + \frac{2}{3}E_q^2\langle r^2 \rangle + \frac{1}{15}E_q^4\langle r^4 \rangle. \quad (24)$$

Since all integrals in these expressions are positive, we recover the limit [14]

$$\xi'(1) < -\frac{1}{2}, \quad (25)$$

and also obtain

$$\xi''(1) > \frac{1}{2} \quad (26)$$

Similar limits can be found for the third and higher order derivatives.

4 Results

The parameters appearing in the spinless RFT model are the string tension a , the short range potential constant κ , and the quark masses. In our calculation, we fix the tension from the universal Regge slope $\alpha' \simeq 0.8 \text{ GeV}^{-2}$,

$$a = \frac{1}{2\pi\alpha'} \simeq 0.2 \text{ GeV}^2. \quad (27)$$

This is consistent with the value found from analyses of heavy onia spectroscopies [12]. We also fix the light quark mass $m_{u,d}$, as the quality of our fit depends only weakly on its value. The remaining parameters κ , m_s , m_c and m_b are varied to best account for the 6 spin averaged states [5, 6]. As an example, in Table 1 we show the results of our fit when $m_{u,d}$ was fixed at 0.3 GeV. Once the parameters of the model are determined, the wave functions and LDF energies E_q are known and the IW function can be calculated with the aid of (21).

The IW function, as computed from (21), is displayed in Fig. 1. The solid and dashed curves correspond to $m_{u,d} = 0$ and 300 MeV respectively. We observe that

with increasing light quark mass the two IW functions differ by only a few percent at $\omega = 1.5$.

One can expand the IW function about zero recoil point as discussed at the end of the preceding section. Using (23) and (24) we have explicitly evaluated the first and second derivatives over the usual range of light quark masses $m_{u,d}$ as shown in Figs. 2 and 3. These derivatives vary by less than ten percent over the range of $m_{u,d}$ and we conclude that

$$\xi'(1) = -0.93 \pm 0.04 , \quad (28)$$

$$\xi''(1) = 1.7 \pm 0.1 . \quad (29)$$

In Fig. 4 we compare the power series approximation about the zero recoil point $\omega = 1$ to the full IW function. We observe that the power series expansion is not very convergent and that a significant error is encountered even including cubic terms in $\omega - 1$ near the high end of the ω range. In particular, if one truncates the series to include only the linear term, then in fitting to the data the slope will be overestimated, i. e. the true slope will be more negative.

The explicit values of the derivatives will provide an excellent test of the RFT model through lattice simulation calculations. It has been proposed [15] that a direct evaluation of higher derivatives of the IW function at zero recoil point is possible by numerical QCD methods.

In Fig. 5 we show the ratio of the IW functions for \bar{B}_s and \bar{B} semileptonic decays. Using light quark mass values $m_s = 513 \text{ MeV}$ and $m_{u,d} = 300 \text{ MeV}$, from the fit of Table 1, we see that the IW function for the two decays differ by less than by 1.5%. We also note that $\xi_{\bar{B}_s}(\omega) \leq \xi_{\bar{B}}(\omega)$.

A comparison of our IW function $\xi_{\bar{B}}(\omega)$ with the recent ARGUS [16] and CLEO II data [17] (shown in Fig. 6) yields the V_{cb} element of the CKM matrix

$$V_{cb} = 0.035 \pm 0.001 \quad (30)$$

(the χ^2 of this fit was 0.88 per degree of freedom). The RFT prediction for the ω dependence of the IW function is in excellent agreement with the data. Finally, using expressions given in [18] for differential widths of \bar{B} and \bar{B}_s decays, we calculate corresponding branching ratios to be

$$Br(\bar{B} \rightarrow D l \bar{\nu}) = 1.79 \left(\frac{\tau_{\bar{B}}}{1.53 ps} \right) \% , \quad (31)$$

$$Br(\bar{B} \rightarrow D^* l \bar{\nu}) = 5.01 \left(\frac{\tau_{\bar{B}}}{1.53 ps} \right) \% , \quad (32)$$

$$Br(\bar{B}_s \rightarrow D_s l \bar{\nu}) = 1.83 \left(\frac{\tau_{\bar{B}_s}}{1.53 ps} \right) \% , \quad (33)$$

$$Br(\bar{B}_s \rightarrow D_s^* l \bar{\nu}) = 5.11 \left(\frac{\tau_{\bar{B}_s}}{1.53 ps} \right) \% . \quad (34)$$

Agreement with the available data [19] for $\bar{B} \rightarrow D$ (1.8 ± 0.4)% and for $\bar{B} \rightarrow D^*$ (4.5 ± 0.4)% is satisfactory. We also find that

$$Br(\bar{B} \rightarrow D l \bar{\nu}) \approx Br(\bar{B}_s \rightarrow D_s l \bar{\nu}) , \quad (35)$$

and

$$Br(\bar{B} \rightarrow D^* l \bar{\nu}) \approx Br(\bar{B}_s \rightarrow D_s^* l \bar{\nu}) . \quad (36)$$

as expected from the heavy-quark symmetry.

Since the IW function is normalized at the zero recoil point to $\xi(1) = 1$, much of the model dependence is distilled into the slope at zero recoil $\xi'(1)$. Various models have yielded a wide range of slopes [20] from $-\frac{1}{3} > \xi'(1) > -2$. Our result for the slope in the RFT model is from (28)

$$\xi'_{\bar{B}}(1) = -0.93 \pm 0.04 , \quad (37)$$

where the error is estimated from the slope dependence on the light quark mass shown in Fig. 2. The recent CLEO II experimental slope value [17] is

$$\xi'_{\bar{B}}(1) = -0.82 \pm 0.12 \pm 0.12 , \quad (38)$$

which is consistent with our predicted value. This value was obtained by assuming $\xi(\omega) \simeq 1 + \xi'(1)(\omega - 1)$. As we have discussed the slope obtained by this truncation will be overestimated, i. e. the actual value should be more negative.

The RFT model must of course agree with experimental data, but it also must be consistent with fundamental results from QCD. The lattice simulation method provides several recent results for $\xi'(1)$. The calculation of Bernard et al. [21] gives

$$\xi'_{\bar{B}}(1) = -1.24 \pm 0.26 \pm 0.33 , \quad (39)$$

while that of Mandula and Ogilvie [22] yields

$$\xi'_{\bar{B}}(1) \simeq -0.95 , \quad (40)$$

and the UKQCD collaboration result [23] is

$$\xi'_{\bar{B}}(1) = -1.2^{+0.7}_{-0.3} . \quad (41)$$

The agreement among these results is a gratifying demonstration of the consistency of the RFT model with QCD.

ACKNOWLEDGMENTS

This work was supported in part by the U.S. Department of Energy under Contract No. DE-AC02-76ER00881 and in part by the University of Wisconsin Research Committee with funds granted by the Wisconsin Alumni Research Foundation.

References

- [1] N. Isgur and M. B. Wise, Phys. Lett. **232B**, 113 (1989); **237B**, 527 (1990).
- [2] Dan LaCourse and M. G. Olsson, Phys. Rev. D **39**, 2751 (1989).
- [3] Collin Olson, M. G. Olsson and Ken Williams, Phys. Rev. D **45**, 4307 (1992).
- [4] M. G. Olsson and Ken Williams, Phys. Rev. D **48**, 417 (1993).
- [5] C. Olson, M. G. Olsson and D. LaCourse, Phys. Rev. D. **49**, 4675 (1994).
- [6] M. G. Olsson and Siniša Veseli, *The Asymmetric Flux Tube*, UW-Madison preprint MAD/PH/816.
- [7] E. Eichten and F. Feinberg, Phys. Rev. D **23**, 2724 (1981); D. Gromes, Z. Phys. C **22**, 265 (1984); **26**, 401 (1984); A. Barchielli, E. Montaldi and G. M. Prosperi, Nucl. Phys. **B296**, 625 (1988); **B303**, 752(E) (1988).
- [8] A. Barchielli, N. Brambilla and G. M. Prosperi, Nuovo Cim **103A**, 59 (1989).
- [9] N. Brambilla and G. M. Prosperi, Phys. Lett. **236B**, 69 (1990).
- [10] W. Buchmüller, Phys. Lett. **112B**, 479 (1982).
- [11] Robert D. Pisarski and John D. Stack, Nucl. Phys. **286B**, 657 (1987).
- [12] Steve Jacobs, M. G. Olsson, and Casimir Suchyta III, Phys. Rev. D **33**, 3338 (1986).
- [13] O. Lie-Svendsen and H. Høgaasen, Z. Phys. C **35**, 239 (1987).
- [14] M. Sadzikowski and K. Zalewski, Z. Phys. C **59**, 677 (1993).
- [15] U. Aglietti, G. Martinelli, and C. T. Sachrajda, Phys. Lett. **B324**, 85 (1994).

- [16] H. Albrecht et al., ARGUS Collaboration, Z. Phys. C **57**, 533 (1993).
- [17] B. Barish et al., CLEO Collaboration, *Measurement of the $\bar{B} \rightarrow D^* l \bar{\nu}_l$ anti-neutrino branching ratios and $|V_{cb}|$* , Cornell Nuclear Studies Wilson Lab preprint, HEPEX 9406005 (1994).
- [18] M. Neubert, Phys. Lett. **264B**, 455 (1991).
- [19] Particle Data Group, Phys. Rev. D **50**, Part I (1994).
- [20] G. V. Efimov et al., Z. Phys. C **54**, 349 (1992); A. V. Radyushkin, Phys. Lett **271B**, 218 (1991).
- [21] C. Bernard, Y. Shen and A. Soni, Phys. Lett **317B**, 164 (1993).
- [22] J. E. Mandula and M. C. Ogilvie *A Lattice Calculation of the Heavy Quark Universal Form Factors*, HEPLAT 9312013 (1993).
- [23] S. P. Booth at al., Phys. Rev. Lett. **72**, 462 (1994).

TABLES

Table 1: Heavy-light spin averaged states. Spin-averaged masses are calculated in the usual way, by taking $\frac{3}{4}$ of the triplet and $\frac{1}{4}$ of the singlet mass.

state	spectroscopic label		spin-averaged	theory	error
	J^P	$^{2S+1}L_J$	mass (MeV)	(MeV)	(MeV)
<u>$c\bar{u}, c\bar{d}$ quarks</u>					
D (1867)	0^-	1S_0			
D^* (2010)	1^-	3S_1	$1S$ (1974)	1975	1
D_1 (2424)	1^+	1P_1	$1P$ (2424)	2425	1
<u>$c\bar{s}$ quarks</u>					
D_s (1969)	0^-	1S_0			
D_s^* (2110)	1^-	3S_1	$1S$ (2075)	2074	-1
D_{s1} (2537)	1^+	1P_1	$1P$ (2537)	2536	-1
<u>$b\bar{u}, b\bar{d}$ quarks</u>					
B (5279)	0^-	1S_0			
B^* (5325)	1^-	3S_1	$1S$ (5312)	5311	-1
<u>$b\bar{s}$ quarks</u>					
B_s (5368)	0^-	1S_0	$1S$ (5409)	5410	1

$$\begin{aligned}
 m_{u,d} &= 300 \quad MeV \quad (\text{fixed}) \\
 m_s &= 513 \quad MeV \\
 m_c &= 1292 \quad MeV \\
 m_b &= 4628 \quad MeV \\
 a &= 0.2 \quad GeV^2 \quad (\text{fixed}) \\
 \kappa &= 0.516
 \end{aligned}$$

FIGURES

Figure 1: IW function for $\bar{B} \rightarrow D^{(*)}l\bar{\nu}_l$ decays for $m_{u,d} = 0$ and $m_{u,d} = 0.3 GeV$ (dashed line).

Figure 2: Slope of the IW function at zero recoil for \bar{B} decays as a function of $m_{u,d}$.

Figure 3: Second derivative of the IW function at zero recoil for \bar{B} decays as a function of $m_{u,d}$.

Figure 4: Power series expansion about $\omega = 1$ (zero recoil point) truncated at various number of terms. The solid curve is the full IW function for \bar{B} decays. In this figure we have taken $m_{u,d} = 0.3 MeV$.

Figure 5: Ratio of $\xi_{\bar{B}_s}$ and $\xi_{\bar{B}}$ for the particular choice of $m_{u,d} = 300 MeV$. The mass of the strange quark was $m_s = 513 MeV$ as a result of the fit of Table 1. We observe the two IW functions differ by less than two percent over the kinematically allowed range of ω .

Figure 6: Comparison of the IW function $\xi_{\bar{B}}(\omega)$ calculated from the RFT model for the particular choice of $m_{u,d} = 300 MeV$ with ARGUS [16] and CLEO II data [17] for the decay $\bar{B}^0 \rightarrow D^{*+}l^-\bar{\nu}_l$. For the sake of clarity, error bars are shown only for the CLEO II data.

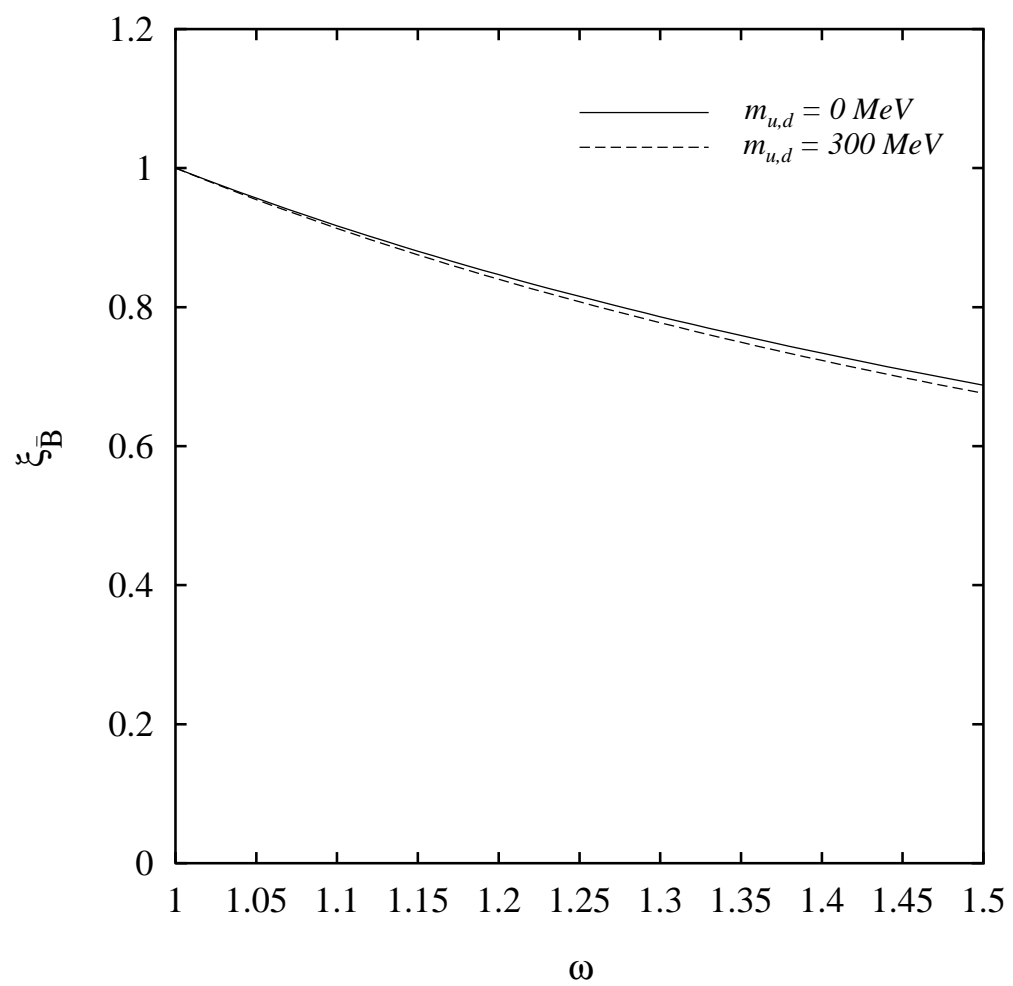


Figure 1

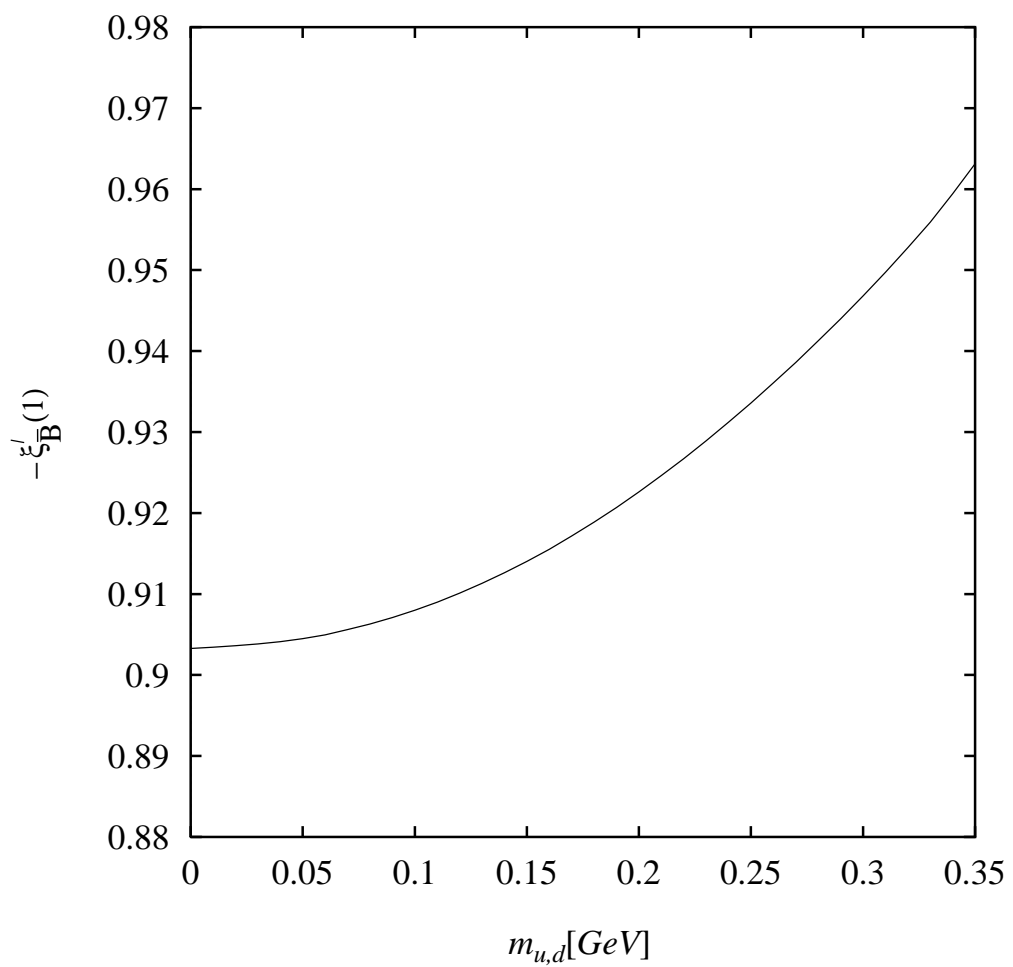


Figure 2

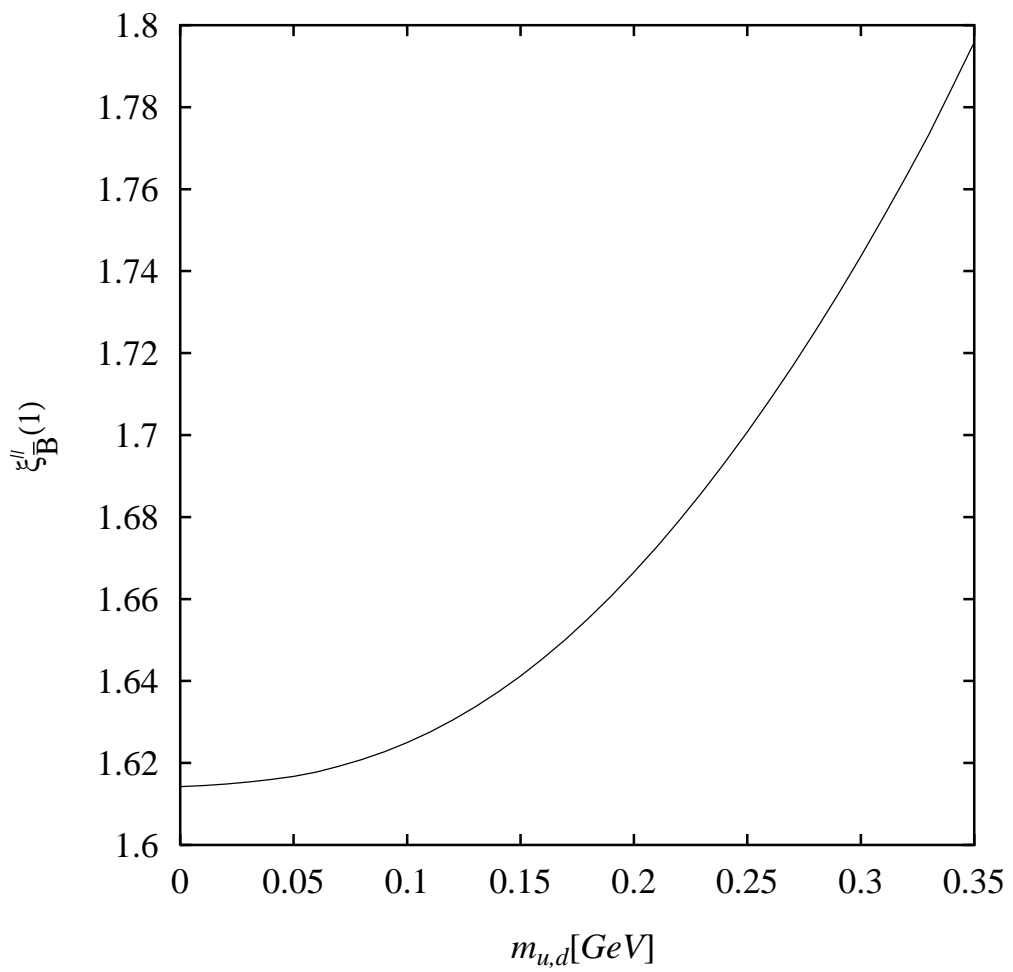


Figure 3

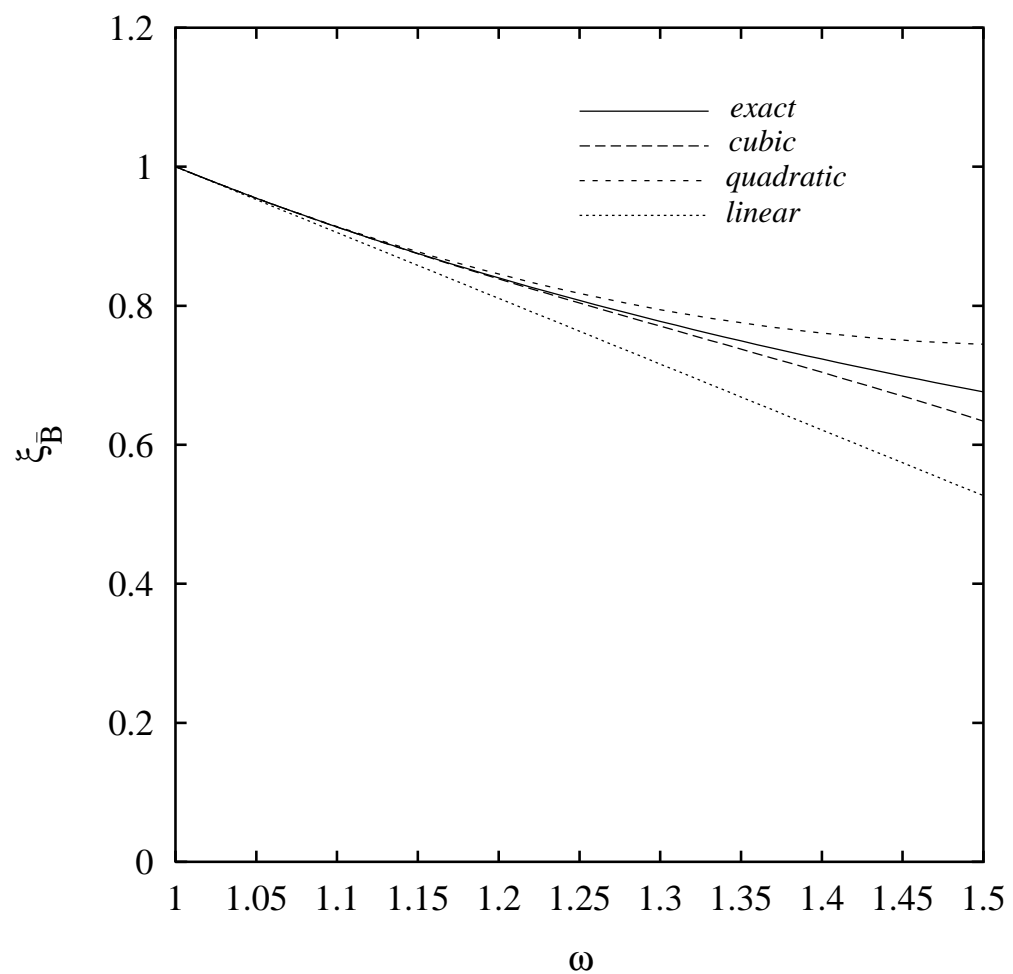


Figure 4

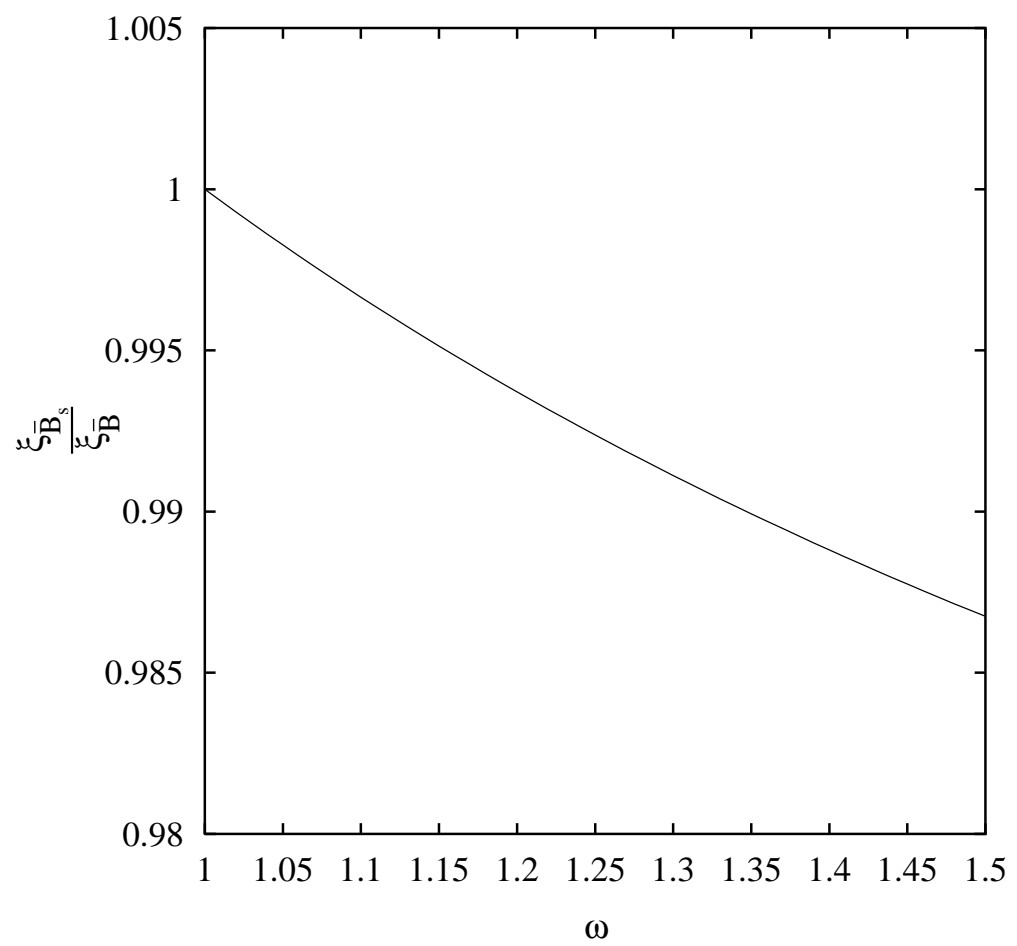


Figure 5

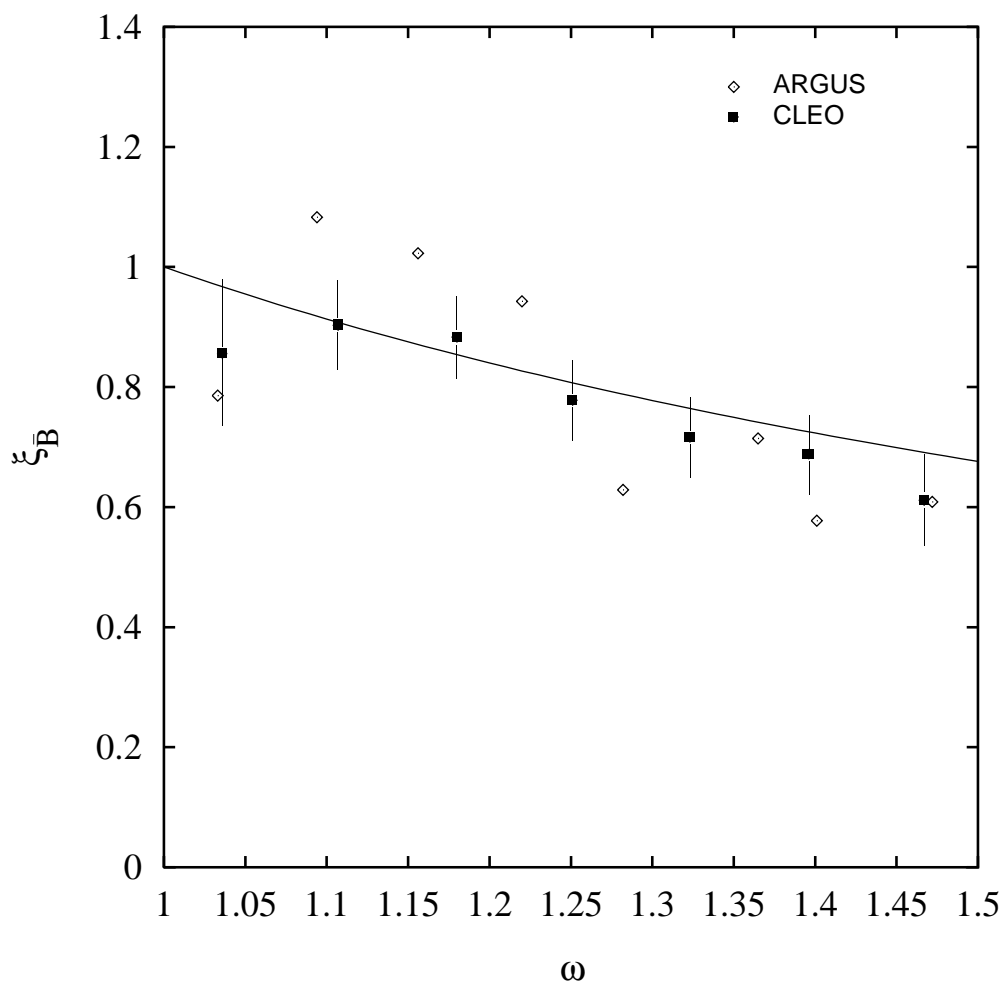


Figure 6